25th ABCM International Congress of Mechanical Engineering
October 20-25, 2019, Uberlândia, MG, Brazil

COB-2019-0329
INFLUENCE OF THE OIL SUPPLY CONDITIONS ON THE STATIC AND DYNAMIC CHARACTERISTICS OF JOURNAL BEARINGS.

Barbara Zaparoli Cunha
Gregory Bregion Daniel
School of Mechanical Engineering, University of Campinas, Rua Mendeleyev 200, Campinas, SP 13083860, Brazil
barbarazaparoli@gmail.com; gbdaniel@fem.unicamp.br;

Abstract. *This paper aims to evaluate the effects of the lubricant feeding conditions on the static and dynamic characteristics of journal bearings. For this, a mass-conserving cavitation model is applied in order to predict the hydrodynamic bearing performance for several oil inlet parameters, such as groove location, number of grooves and feeding pressure. Based on the results obtained by numerical simulations, the oil supply conditions affect the bearing flow rate, the load capacity, the dynamic coefficients and the whirl frequency ratio. As contribution of this paper, the results allow to recognize when oil inlet parameters are relevant to the bearing design, being that the groove position was found to be more significant than feeding pressure, influencing even the unstable behavior of the bearing system.*

Keywords: *hydrodynamic journal bearing, supply conditions, mass-conserving cavitation model, groove parameters, dynamic coefficients.*

1. INTRODUCTION

Hydrodynamic journal bearings are commonly used in mechanical systems in order to support rotating shafts, especially in rotors that operate at high speeds or with high loads. Thus, this kind of bearing directly influences the dynamic behavior and performance of the rotors, since the lubricant not only generates the lifting force but also reduces friction, wear and heating in the machine parts.

Many studies have been carried out to develop models that represent the operation of hydrodynamic bearings with better accuracy. Thus, the lubricant inlet condition should be considered in these models because it is one of the relevant aspects in the bearing performance. Etsion and Pinkus (1974 and 1975) were one of the earliest to consider the influence of lubricant inlet flow on bearing operation, calculating the position where the film covers the entire bearing width and the effective width of the lubricant film before this point.

In order to realistically describe the flows in the bearing, the algorithm proposed by Elrod and Adams (1974) and improved by Elrod (1981) can be applied, since it ensures mass conservation throughout bearing since it takes into account the rupture and reformation boundaries using the Jakobsson-Floberg-Olsson (JFO) cavitation theory. Claro and Miranda (1993), Downson et al. (1985a), Pierre and Fillon (2000) and Brito et al. (2013) applied this algorithm to evaluate the influence of the oil supply condition on the bearing operation. These influences were also studied by Vijayaraghavan and Keith (1992) and Vincent et al. (1995) using a modified shear flow term proposed by Vijayaraghavan and Keith (1989) to obtain a proper differentiation method that improves the convergence of the Elrod algorithm. In general, these works show that the oil inlet parameters, such as the feeding pressure and groove position and geometry, affect the film reformation, power loss, oil flow rate and load capacity. Experimental works (Downson et al., 1985b; Costa et al., 2000; Costa et al., 2003; Brito et al., 2007) agree with the behavior predicted in theory.

The previously mentioned works evaluate the influence of the oil supply conditions on the static characteristics of the bearing. However, there is a lack of studies in literature related to the influence of the oil inlet conditions on the dynamic characteristics of the hydrodynamic bearing, mainly in the dynamic coefficients and whirl frequency ratio, since these parameters affect directly the dynamic behavior of the rotating system.

In this context, the current work undertakes a parametric study to evaluate the influence of oil supply pressure, groove position and number of grooves on the static and also on the dynamic characteristics of hydrodynamic journal bearing. The numerical analyses of the hydrodynamic pressure and flows in the bearing were performed using the Elrod algorithm with the modifications proposed by Vijayaraghavan and Keith (1989). The dynamic characterization of the bearing was evaluated by the linearized stiffness and damping coefficients and the instability threshold was analyzed by the whirl frequency ratio (WFR) of the bearings, as proposed by Lund (1964, 1987) and Lund and Saibel (1967). Thus, the effects of the oil supply conditions on the pressure distribution, flowrate, eccentricity, dynamic coefficients and instability threshold can be evaluated for different operational conditions of the bearing. The results obtained represent important

contributions related to the improvement of the oil inlet conditions in order to guarantee a safe operational condition on the bearing.

2. METODOLOGY

2.1 Governing Equations

The classical Reynolds equation (1886) aims to model the hydrodynamic pressure in the oil film thickness of the hydrodynamic bearing, considering the lubricant oil as incompressible, isoviscous, Newtonian and with inertial forces neglected. Reynolds equation takes the form:

$$\frac{\partial}{\partial x}\left(\frac{h^3}{12\mu}\frac{\partial p}{\partial x}\right)+\frac{\partial}{\partial z}\left(\frac{h^3}{12\mu}\frac{\partial p}{\partial z}\right)=\frac{\partial}{\partial x}\left(\frac{U}{2}h\right)+\frac{\partial h}{\partial t} \tag{1}$$

Where x and z are, respectively, the circumferential and axial coordinates, μ is the dynamic viscosity of the fluid, $h(x)$ is the film thickness, $p(x,z)$ is the pressure distribution in the fluid, U is the linear speed of the shaft surface and t is the time. However, Reynolds equation does not ensure mass conservation in the cavitated region and does not take into account the oil inlet boundary condition, since the bearing is considered as flooded. Therefore, the classical Reynolds model is not appropriate to realistically predict the lubricant flow at inlet.

The mass-conservative equation developed by Elrod and Adams (1974) is valid to both full-film and cavitated regions and implicitly considers the film reformation and cavitation boundaries. The Elrod and Adams model introduces the variable θ that represents the liquid fraction in the cavitated region (volumetric fraction of the bearing gap that is occupied by the lubricant) and the relative density of the lubricant in the full film region (ρ/ρ_c). Moreover, the lubricant compressibility is also considered through the Bulk Modulus (β), as presented in Eq. (2):

$$\beta=\rho\frac{\partial p}{\partial \rho}=\theta\frac{\partial p}{\partial \theta}\quad (full\ film\ region) \tag{2}$$

In order to automatically consider both full and cavitated film on the bearing, a switch function g is assumed from the variable θ as following:

$$g=\begin{cases} 1\ when\ \theta\geq 1\ \ (full\ film\ region) \\ 0\ when\ \theta<1\ \ (cavitated\ region)\end{cases} \tag{3}$$

From Eq. (2) and Eq. (3) it is possible to relate the partial derivatives of pressure with partial derivatives of θ:

$$\frac{\partial p}{\partial x_i}=g\frac{\beta}{\theta}\frac{\partial \theta}{\partial x_i} \tag{4}$$

Then, Reynolds equation can be rewritten in relation to θ, resulting in the "universal" equation proposed by Elrod and Adams (1974):

$$\frac{\partial}{\partial x}\left(\frac{h^3}{12\mu}g\beta\frac{\partial \theta}{\partial x}\right)+\frac{\partial}{\partial z}\left(\frac{h^3}{12\mu}g\beta\frac{\partial \theta}{\partial z}\right)=\frac{\partial}{\partial x}\left(\frac{U}{2}h\theta\right)+\frac{\partial(h\theta)}{\partial t} \tag{5}$$

The terms on the left side are the pressure-induced flow in circumferential and axial directions, known as Poiseuille flows, while the first term on the right side is the shear flow term, known as Couette flow, and the second term is the Squeeze flow term. Equation (5) assumes an elliptic form in full film region ($g=1$), where it behaves as Reynolds equation, and it has a hyperbolic form in cavitated region ($g=0$).

2.2 Numerical Procedure

Integrating the Eq. (5) along a control volume P leads to the flow balance presented:

$$Q^e_{Poi}-Q^w_{Poi}+Q^n_{Poi}-Q^s_{Poi}=Q^e_{Cou}-Q^w_{Cou}+Q_{sq} \tag{6}$$

Where the superscripts e, w, n, s indicate the east, west, north and south borders, respectively. Equation (7) shows the Poiseuille flow in eastern boundary to exemplify the calculation of the pressure induced flow, as proposed by Elrod (1981).

$$Q^e_{Poi}=\left(\beta\Delta z\frac{h_e^3}{12\mu}\right)g\frac{\partial \theta}{\partial x}\bigg|_e=\left(\beta\Delta z\frac{h_e^3}{12\mu}\right)\frac{g_E(\theta_E-1)-g_P(\theta_P-1)}{\Delta x} \tag{7}$$

This formulation ensures the pressure induced flow in the full film region but it is vanished in the cavitated region, guaranteeing the mass conservation in the boundaries between both regions as proposed by JFO boundary condition.

The convective term will be treated as proposed by Vijayaraghavan and Keith (1989), that inserted an artificial viscosity in the Couette term to account for compressibility effects, which leads to:

$$Q_{Cou}^{e} = \Delta z \frac{U}{2}\left(\theta h - \mu_a \frac{\theta h}{\partial x}\frac{\Delta x}{2}\right)_e = \Delta z \frac{U}{2}\left(\frac{\theta_P h_P + \theta_E h_E}{2} - \frac{\mu_E + \mu_P}{2}\frac{(\theta_E h_E - \theta_P h_P)}{\Delta x}\frac{\Delta x}{2}\right) \quad (8)$$

The formulation presented in Eq. (7) and Eq. (8) for the Poiseuille and Couette flows at the eastern boarder can be generalized to the other boarders and replaced in Eq. (6). The Squeeze term is explicitly evaluated in the volume centroid as:

$$Q_{sq} = h_P \frac{\partial \theta_P}{\partial t}\Delta x \Delta z + \theta_P V_P \Delta x \Delta z \quad (9)$$

Where V_P is the translational speed of the shaft surface at control volume *P*. This approach results in a discretization method with central differentiation in the full film region and upwind differencing in the cavitated region, which is appropriate to solve Eq. (5).

When the algorithm is applied to the entire mesh of control volumes, the result is a system of equations which variables are the values of θ for each volume and that will be dependent only on the values of the neighboring volumes. This system of equations can be solved by the Gauss-Seidel method, updating the values of θ and g in each step until the system converges. There are basically two boundary conditions in the system: ambient pressure at the bearing sides and feeding pressure P_f in the grooves. The relation between θ and the pressure can be found by integrating Eq. (2) to yield:

$$p = p_c + g\beta\, ln(\theta) \approx p_c + g\beta(\theta - 1) \quad (10)$$

The approximation in Eq. (10) is valid because θ assumes values slightly greater than 1 in the full film region. An algebraic manipulation of Eq. (10) leads to the value of θ corresponding to a given pressure, which is used to impose the boundary conditions on the sides of the bearing and in the grooves.

Finally, the hydrodynamic forces acting in the journal are evaluated by the integration of the pressure field along the bearing area, as presented by:

$$F_X = \int_0^{2\pi R}\int_0^{L} P(x,z)\cos(x/R)\, dzdx = \sum_{i=1}^{N_x}\sum_{j=1}^{N_z} P_{i,j}\cos(x_i/R)\,\Delta x \Delta z \quad (11)$$

$$F_Y = \int_0^{2\pi R}\int_0^{L} P(x,z)\sin(x/R)\, dzdx = \sum_{i=1}^{N_x}\sum_{j=1}^{N_z} P_{i,j}\sin(x_i/R)\,\Delta x \Delta z \quad (12)$$

In order to satisfy the forces balance inside the bearing, the equilibrium position of the shaft is found for the static case ($\partial/\partial t=0$) using the Newton-Raphson method. These hydrodynamic forces have a linear behavior close to the equilibrium position and, therefore, they can be represented using linear coefficients, as proposed by Lund (1964, 1987). The stiffness and damping coefficients of the bearing are equivalent to the partial derivatives evaluated at the equilibrium position:

$$K_{uv} = \left.\frac{\partial F_u}{\partial v}\right|_0; \qquad C_{uv} = \left.\frac{\partial F_u}{\partial \dot{v}}\right|_0; \quad (13)$$

Where u and v represent the translational coordinates of the shaft inside the bearing (x and y directions). Finite perturbations are applied at the position and velocity of the shaft in order to solve the partial derivatives of Eq. (13) using the centered differences method. The variation of θ with respect to time is disregarded (expansion term), since the transient effects of the volumetric fraction are not considered in this linear approach of the hydrodynamic forces. In this way, the first term of Eq. (9) is null.

Lastly, the investigation of the fluid induced instability (oil whirl/whip) was evaluated by the whirl frequency ratio as described by Lund and Saibel (1967) and Lund (1987). This analysis is based on the solution of the eigenvalue problem of the equation of motion of the bearing evaluated in the instability threshold, which leads to the following equations:

$$M_{crit}\omega_0^2 = \frac{K_{xx}C_{yy} + K_{yy}C_{xx} - K_{xy}C_{yx} - K_{yx}C_{xy}}{C_{xx} + C_{yy}} = k_{eq} \quad (14)$$

$$\omega_0^2 = \frac{(K_{xx} - k_{eq})(K_{yy} - k_{eq}) - K_{xy}K_{yx}}{C_{xx}C_{yy} - C_{xy}C_{yx}} \quad (15)$$

Where k_{eq} is the equivalent stiffness and ω_0 is the precession (whirl) frequency of the fluid film. From these equations, the whirl frequency ratio (WFR) can be calculated as:

$$WFR = \frac{\omega_0}{\Omega} \tag{16}$$

From the equivalent stiffness k_{eq} and the rotor mass M, it is possible to obtain the natural frequency ω_n of a symmetric rigid rotor, which can be compared to the whirl frequency ω_0 to establish the instability threshold of the system.

$$\omega_n = \sqrt{\frac{2k_{eq}}{M}} \tag{17}$$

Figure 1 shows the steps applied throughout this paper in order to obtain the static and dynamic characteristic of the bearing under different supply conditions.

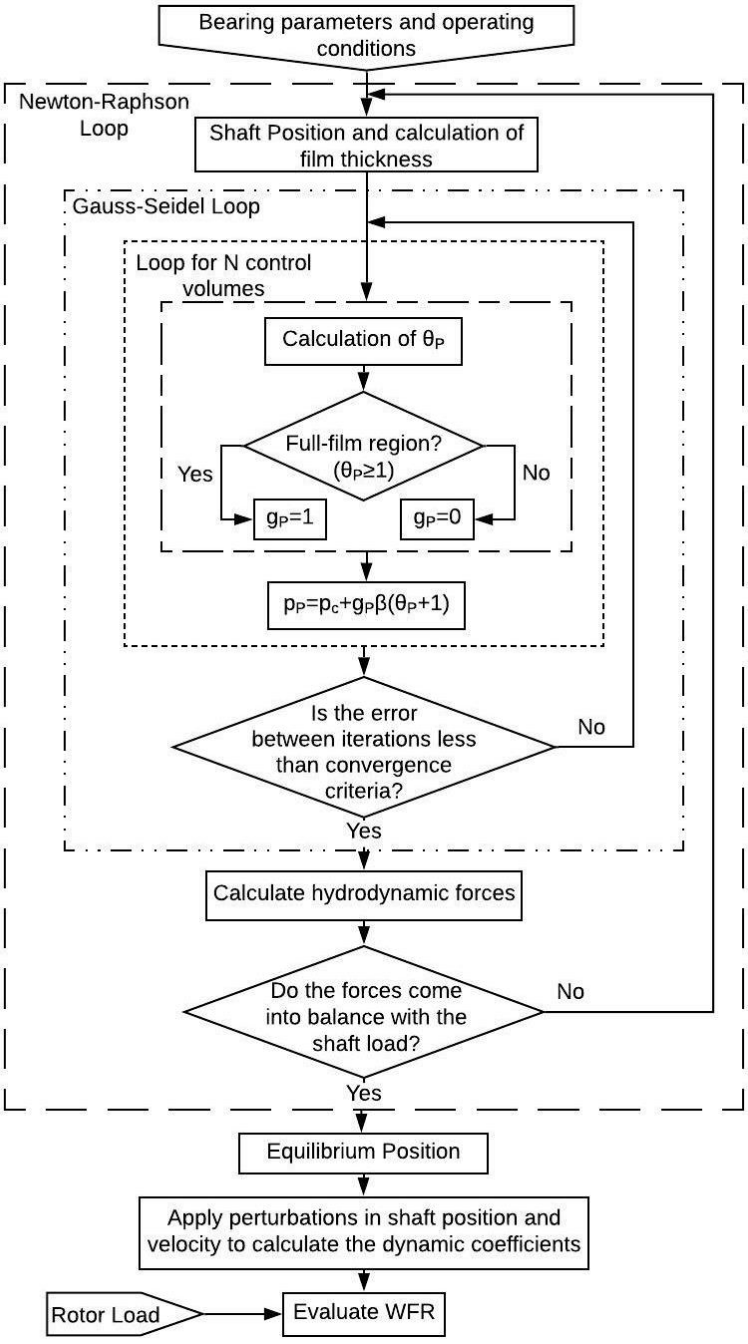

Figure 1. Flowchart of the numerical procedure used in this work.

3. RESULTS

The methodology presented in previous section was applied in order to verify the influence of the effects of the oil supply conditions on the hydrodynamic behavior of the journal bearing. The hydrodynamic journal bearing considered in the computational simulations has a diameter of 50 mm, width of 30 mm, radial clearance of 80 μm and the lubricant oil used in the bearing has dynamic viscosity of 0.04 Pa.s. A parametric study related to the effects of the oil supply conditions on bearing performance was carried out considering a load of 500 N on the bearing and the rotor's rotation range from 1 to 150 Hz. The grooves considered in all simulations have a width of 21mm and length of 5 mm.

3.1 Effects of the Feeding Pressure

Figure 2 shows the influence of the feeding pressure P_f on shaft's locus and on bearing's flowrates when the groove is located 90° from the load line. In this case, the supply pressure does not strongly influence the bearing load capacity when considering feeding pressures lower than 10 kPa. However, the load capacity increases significantly for inlet pressures as high as 100 kPa. As expected, Fig. 2b shows that the inlet flowrate arises as the supply pressure and the rotation speed arise. Moreover, the inlet flowrates Q_{in} are similar the side leakages Q_{out}, showing consistency with the mass conservative principle. The difference in the hydrodynamic pressure field for supply pressure equals 0 Pa and 100 kPa is shown in Fig. 2c and Fig. 2d, respectively, evidencing the feeding pressure in the groove region.

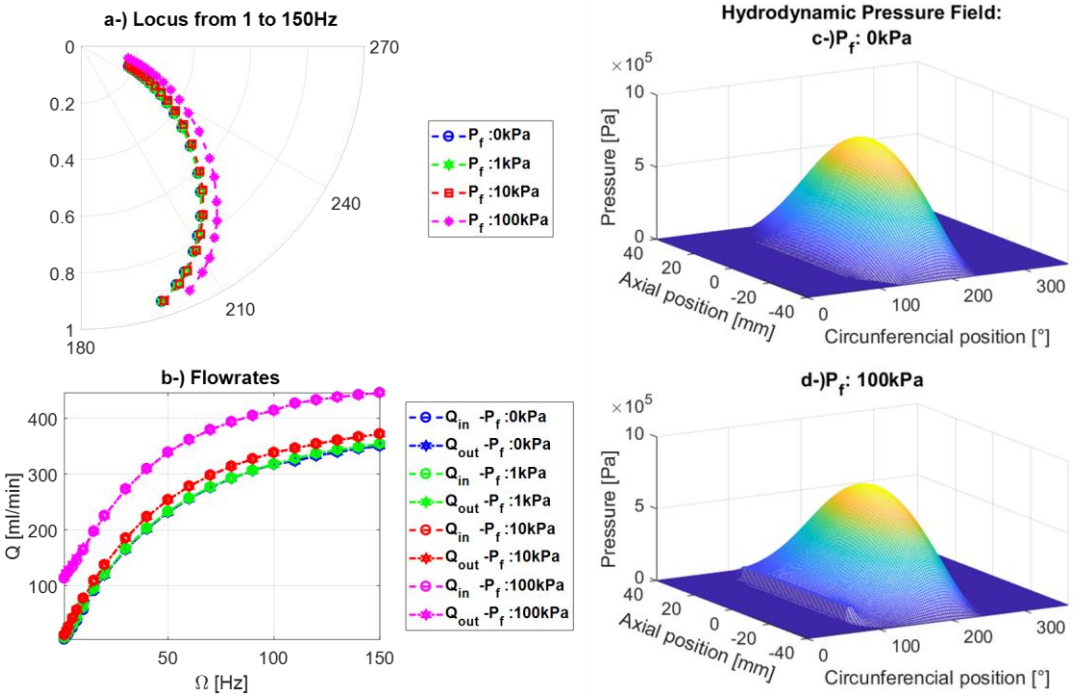

Figure 2. Analysis of the influence of feeding pressure in the shaft locus (a), in the flowrates (c) and in the hydrodynamic pressure field for rotation speed of 50Hz for $P_f = 0$ *Pa* (b) and $P_f = 10^5$ *Pa* (d).

The equivalent stiffness and damping coefficients do not change significantly with the feeding pressure, as observed respectively in Fig. 3 and Fig. 4, except for the coefficient K_{xx} that increases with P_f once that the feeding pressure acts directly in this direction. It should be noted that all graphs from this work showing the dynamic results were plotted for rotation speed from 10 to 150 Hz in order to improve the visualization.

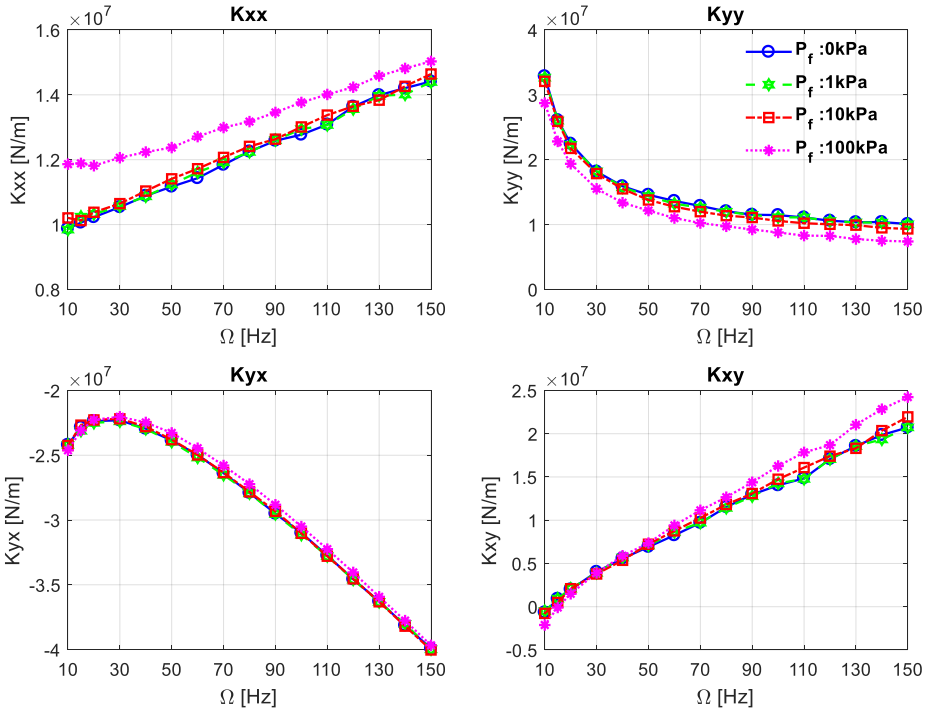

Figure 3. Influence of the feeding pressure in the equivalent stiffness coefficients.

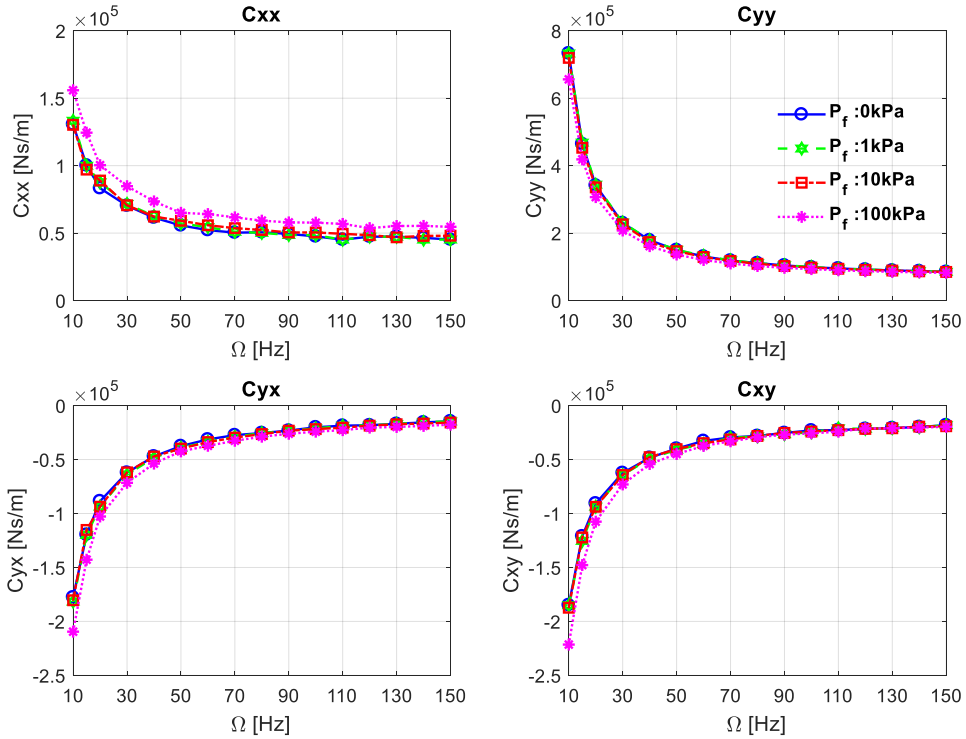

Figure 4. Influence of feeding pressure in the equivalent damping coefficients.

According to Fig. 5, the WFR value approaches 0.5 for all feeding pressures. As pointed out by Lund (1987), this value is typical of cylindrical hydrodynamic bearings and it indicates that the rotor becomes unstable when the rotation is approximately equal to twice the natural frequency of the system. This instability threshold can be seen in Fig. 5b as the intersection of the whirl and natural frequencies, being in agreement with the observation above.

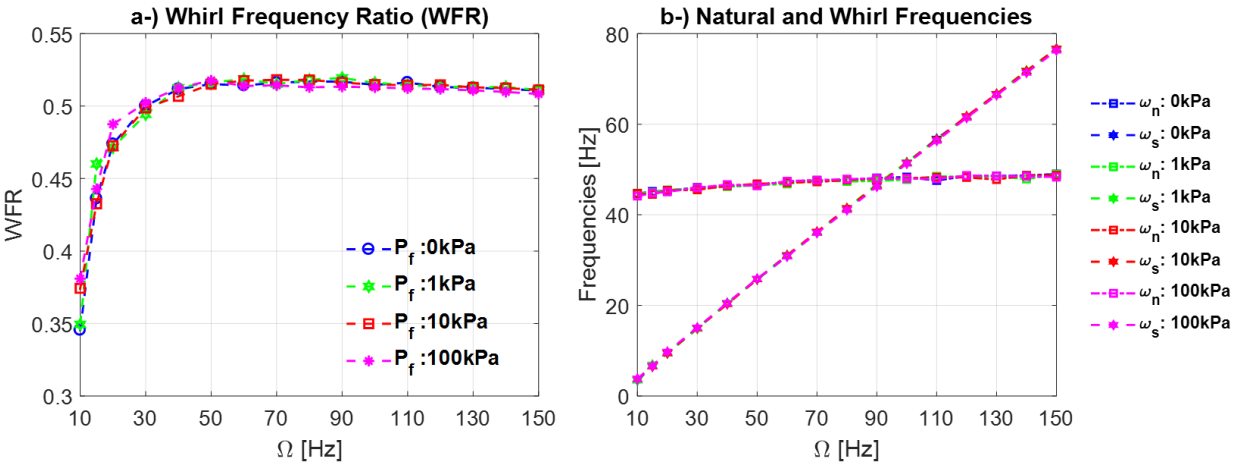

Figure 5. Influence of feeding pressure in the whirl frequency ratio (a) and in the whirl and natural frequencies (b).

3.2 Effects of the Groove Position

The effects of the groove position were analyzed for four different cases: groove at 0° or in the load line; 90° from the load line; 270° from load line; and a bearing with two grooves, one at 90° and another at 270º, as can be seen in Fig. 6. Figure 7 compares the locus of the shaft and the hydrodynamic pressure distribution for all these groove positions. According to Fig. 7a and d, the configuration with two grooves and the one with one groove at 90° position lead to the same behavior for lubricant flowrates and shaft equilibrium position. In all cases, a single groove at 270° results in higher eccentricities and much smaller lubricant flowrates. The peak pressure in the bearing with one groove at 270° also is higher than in other configurations, as observed in Fig. 7b, c, e and f. Thus, special attention must be taken for bearing in which the journal rotation can be reversed, since the groove at 90° can operate as a groove at 270°.

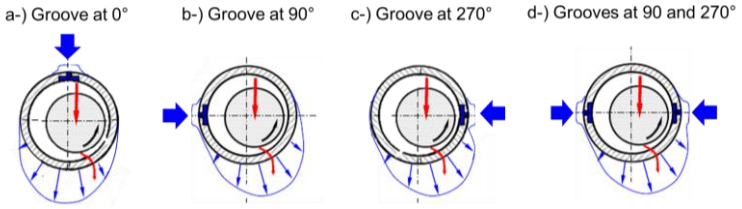

Figure 6. Illustration of the cases of groove position: (a) at 0°; (b) at 90; (c) at 270º; (d) at 90° and 270°.

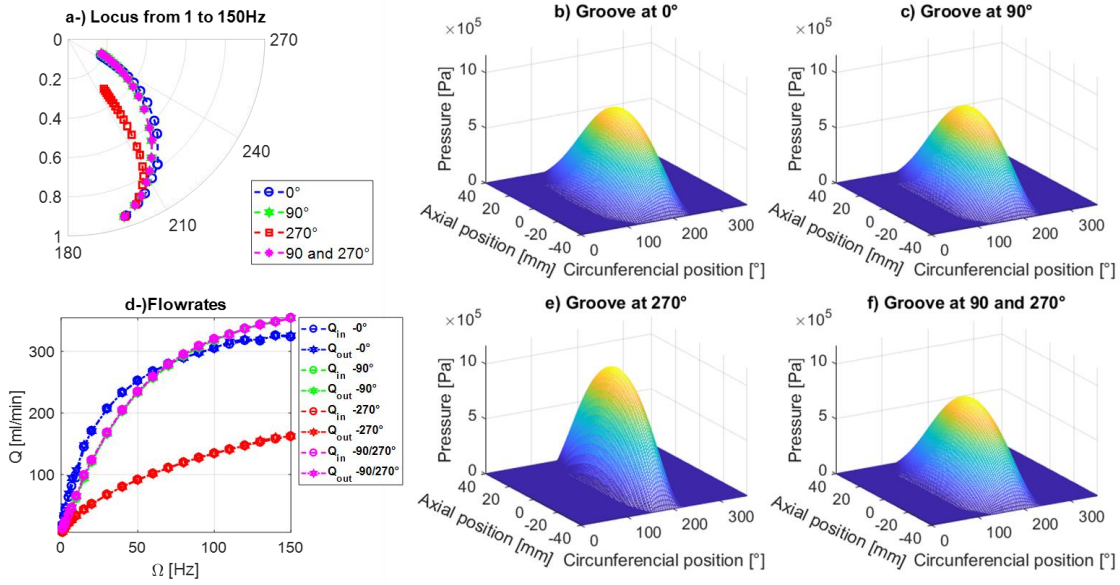

Figure 7. Effects of the groove position in the shaft locus (a), flowrate (d) and in the hydrodynamic pressure distribution (b, c, e and f) for a bearing with load of 500 N and supply pressure of 1 kPa.

Figures 8 and 9 show respectively the stiffness and the damping coefficients evaluated for all groove positions. Once again, the results are equivalent for the bearing with grooves at 90° and 270° and the one with one groove at 90°. It can also be observed that the equivalent stiffness coefficients of the bearing with groove at 270° behave substantially different from the others.

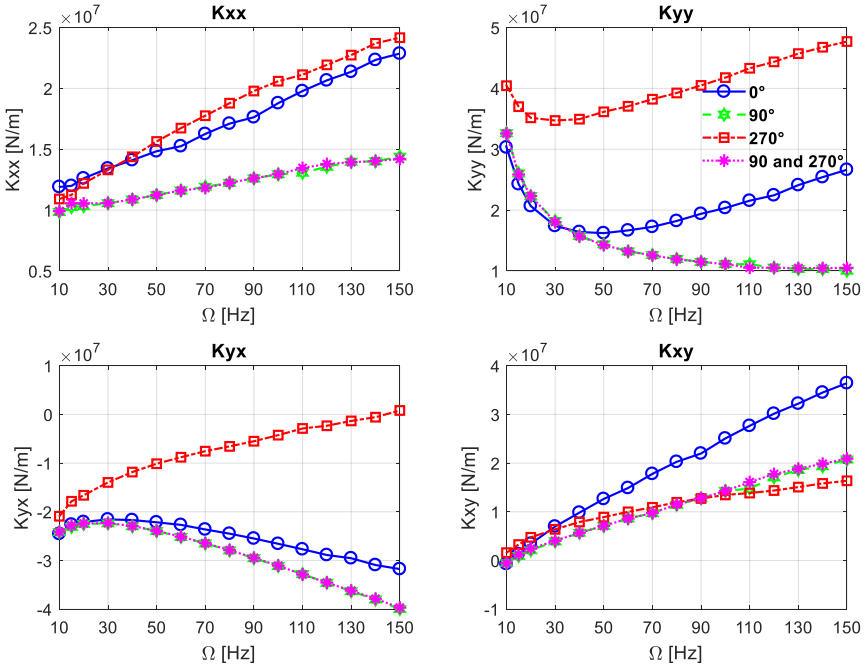

Figure 8. Effects of the groove position in the stiffness coefficients.

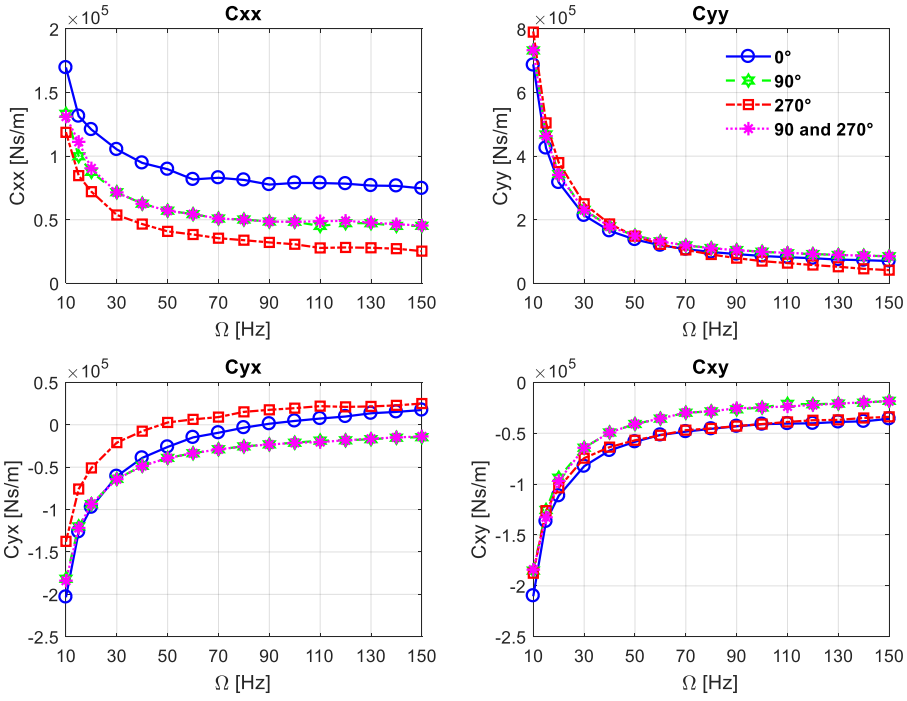

Figure 9. Effects of the groove position in the damping coefficients.

Figure 10a shows that the WFR values are around 0.5 for all bearings, except for the bearing with groove at 270°. In this case, the WFR values decrease as the rotational speed increases, being equal to zero for rotations higher than 110 Hz, indicating that no whirl occurs. As the position of the groove influences the dynamic coefficients, consequently the equivalent coefficient k_{eq} and the natural frequency ω_n will also be influenced, as can be seen in Fig. 10b. Besides that,

Fig. 10b indicates that the instability threshold is close to 90Hz for the bearing with groove at 90° and the bearing with two grooves, while it is close to 110Hz for the groove at 0°. The bearing with groove at 270° behaves always stable, which can be explained by its high eccentricities and smaller cross-coupled stiffness coefficients in comparison to the other configurations.

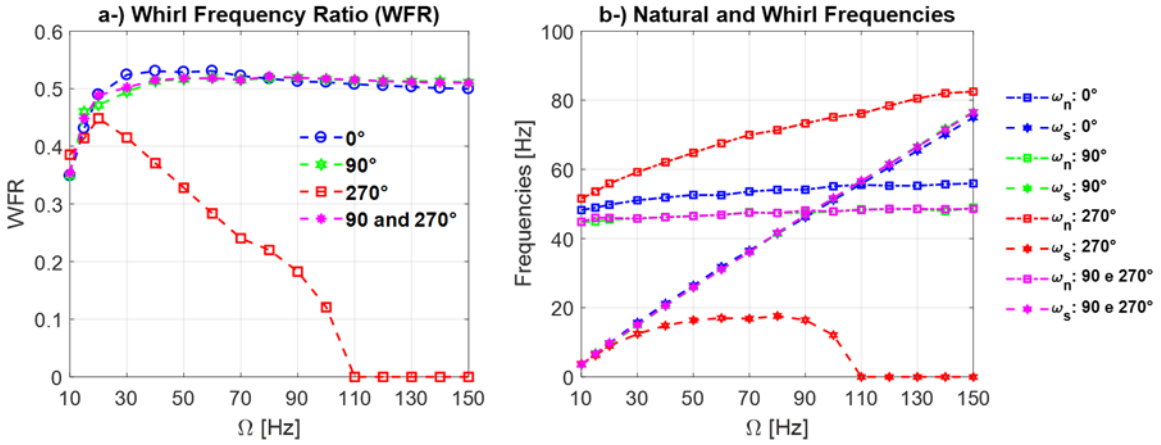

Figure 10. Influence of the groove position in the whirl frequency ratio (a) and in the whirl and natural frequencies (b).

It is important to point out that the instability analysis presented in this paper applies to a rigid and symmetrical rotor and, therefore, it aims to analyze only the influence of the bearing on the dynamic behavior of the system. In order to analyze the stability of the complete system it is necessary to also consider the flexibility of the rotor, therefore further studies should be done to consider the effects of the bearing supply conditions on flexible rotors.

4. CONCLUSIONS

This work presents a model of hydrodynamic lubrication for the evaluation of the influence of the oil supply conditions in both static and dynamic performance of the bearing. The results show that the effects of the feeding pressure are notable only for pressures greater than 100 kPa, when the load capacity rises. The oil flowrates analyses show that the model is in fact conservative, since the inlet flowrate is equal the side leakage. Moreover, the inlet flow increases as the rotational speed and the feeding pressure also increase. The WFR analyses show that the instability occurs when the rotation speed reaches twice the system natural frequency for all feeding pressures simulated, as commonly seen in cylindrical hydrodynamic bearings.

On the other hand, distinct groove positions result in very different lubrication conditions, as evidenced by the different lubrication flowrates obtained. Consequently, all results showed to be strongly dependent on this parameter. This is clear on the analysis of the bearing with one groove at 270°, which behaves remarkably distinct from the others, leading to higher pressure peaks, lower bearing capacities and flowrates and to an always stable system, while the other groove positions presented the usual value of the whirl frequency ratio equal to 0.5. In addition, it is noted that bearings with one groove at 90° and bearings with two grooves, at 90° and 270°, present a similar behavior.

Therefore, the results show that oil inlet parameters, mainly the groove position, have a great impact on the static and dynamic performance of the bearing, being it possible to affect the dynamic behavior of rotating system. For this reason, the evaluation of the oil supply conditions is relevant for the proper design of hydrodynamic bearings used in industrial applications.

5. ACKNOWLEDGEMENTS

This study was financed in part by the Coordenação de Aperfeiçoamento de Pessoal de Nível Superior - Brasil (CAPES) - Finance Code 001. The authors would also like to thank the FAPESP (grant 2015/20036-5) and CNPq for supporting this research.

6. REFERENCES

Brito, F. P., Miranda, A. S., Claro, J. C. P., Teixeira, J. C., Costa, L., and Fillon, M., 2014. “The role of lubricant feeding conditions on the performance improvement and friction reduction of journal bearings”. Tribology International, Vol. 72, pp. 65-82.

Brito, F. P., Miranda, A. S., Bouyer, J., and Fillon, M., 2007. “Experimental investigation of the influence of supply temperature and supply pressure on the performance of a two-axial groove hydrodynamic journal bearing”. Journal of Tribology, Vol. 129, No. 1, pp. 98-105.

Claro, J. C. P., and Miranda, A. A. S., 1993. “Analysis of hydrodynamic journal bearings considering lubricant supply conditions.” Proceedings of the Institution of Mechanical Engineers, Part C: Journal of Mechanical Engineering Science, Vol. 207, No. 2, pp. 93-101.

Costa, L., Fillon, M., Miranda, A. S. and Claro, J. C. P., 2000. “An experimental investigation of the effect of groove location and supply pressure on the THD performance of a steadily loaded journal bearing.” Trans. ASME, J. Tribology, Vol. 122, pp. 227-232.

Costa, L., Miranda, A. S., Fillon, M., and Claro, J. C. P., 2003. “An analysis of the influence of oil supply conditions on the thermohydrodynamic performance of a single-groove journal bearing”. Proceedings of the Institution of Mechanical Engineers, Part J: Journal of Engineering Tribology, Vol. 217, No. 2, pp. 133-144.

Dowson, D., Taylor, C. M., and Miranda, A. A. S, 1985a. “The Prediction of Liquid Film Journal Bearing Performance with a Consideration of Lubricant Film Reformation: Part 1: Theoretical Results”. Proceedings of the Institution of Mechanical Engineers, Part C: Journal of Mechanical Engineering Science, Vol. 199, No. 2, pp. 95-102.

Dowson, D., Taylor, C. M., and Miranda, A. A. S, 1985b. “The Prediction of Liquid Film Journal Bearing Performance with a Consideration of Lubricant Film Reformation: Part 2: Experimental Results”. Proceedings of the Institution of Mechanical Engineers, Part C: Journal of Mechanical Engineering Science, Vol. 199, No. 2, pp. 103-111.

Elrod, H. G. and Adams, M. L., 1974. "A Computer Program for Cavitation and Starvation Problems". Leeds-Lyon Conference on Cavitation, Leeds Univ. England, pp. 37-41.

Elrod H.G, 1981. “A Cavitation Algorithm”. ASME. Journal of Lubrication Tech, Vol. 103, No. 3, pp. 350-354.

Etsion, I., and Pinkus, O., 1974. "Analysis of short journal bearings with new upstream boundary conditions". Journal of Lubrication Tech, Vol. 96, No. 3, pp. 489-496.

Etsion, I. and Pinkus, O., 1975. “Solutions of Finite Journal Bearings with Incomplete Films”. Journal of Lubrication Technology, Vol. 97, pp. 89-93.

Lund, J. W., 1964. “Spring and damping coefficients for the tilting-pad journal bearing”. ASLE transactions, Vol. 7, No. 4, pp. 342-352.

Lund, J. W. and Saibel, E., 1967. "Oil whip whirl orbits of a rotor in sleeve bearings." Journal of Engineering for industry, Vol. 89, No. 4, pp. 813-823.

Lund, J. W., 1987. Review of the concept of dynamic coefficients for fluid film journal bearings. Journal of Tribology, Vol. 109, No. 1, pp. 37-41.

Pierre, I., and Fillon, M., 2000. “Influence of geometric parameters and operating conditions on the thermohydrodynamic behaviour of plain journal bearings”. Proceedings of the Institution of Mechanical Engineers, Part J: Journal of Engineering Tribology, Vol. 214, No.5, pp. 445-457.

Reynolds, O., 1886. "On the Theory of Lubrication and Its Application to Mr. Beauchamp Tower's Experiments, Including an Experimental Determination of the Viscosity of Olive Oil”. Philosophical Transactions of the Royal Society of London, Vol. 1, pp. 157.

Vijayaraghavan, D., and Keith Jr, T. G., 1989. “Development and Evaluation of a Cavitation Algorithm”. Tribology Transactions, Vol. 32, No.2, pp. 225-233.

Vijayaraghavan, D., and Keith Jr, T. G., 1992. “Effect of type and location of oil groove on the performance of journal bearings”. Tribology transactions, Vol. 35, No. 1, pp. 98-106.

Vincent, B., Maspeyrot P., and Frene J., 1995. "Starvation and cavitation effects in finite grooved journal bearing." Tribology Series. Vol. 30, pp. 455-464.

7. RESPONSIBILITY NOTICE

The authors are the only responsible for the printed material included in this paper.